Enhancement of Sensing Properties of Thin Poly(Methyl Methacrylate) Films by VUV Modification

Ioannis Raptis [1], Janez Kovač[2], Margarita Chatzichristidi [1], Evangelia Sarantopoulou[3*], Zoe Kollia[3], Spomenka Kobe [4], Alkiviadis Constantinos Cefalas[3],

[1]*Institute of Microelectronics, NCSR 'Demokritos', 15310 Agia Paraskevi, Athens ,Greece*
[2] *Department of Surface Engineering and Optoelectronics -F4, Jožef Stefan Institute, Teslova 30, 1000 Ljubljana, Slovenia*
[3] *National Hellenic Research Foundation, TPCI, 48 Vas. Constantinou Aven. Athens 11635 Greece*
E-mail: esarant@eie.gr
[4]*Department of Nanostructured Materials, Jožef Stefan Institute, Jamova 39, SI-1000 Ljubljana, Slovenia*

Surface modification of polymeric films by VUV light is an efficient method to tailor its properties and functionality for a variety of applications. Laser irradiation at 157 nm of poly(methyl methacrylate) (PMMA) thin films deposited on SiO_2 layer, demonstrates a considerable increase of surface and bulk swelling during water vapour sorption in comparison to the non irradiated film areas. AFM images of surface morphology of the irradiated areas reveal that surface roughness depends on the irradiation conditions. Besides morphological changes, X-ray photoelectron spectroscopy (XPS) suggests chemical modification of the irradiated film areas. The enhanced surface swelling and the chemical modification increases the detection efficiency of water analyte in gas phase by many orders of magnitude. This method can be used to fabricate a polymer based sensor array and to engineer its detection efficiency.

DOI: 10.2961/jlmn.2007.03.0007

Keywords: Polymer sensors, PMMA, polymer swelling, laser polymer surface modification, nanostructures, VUV, 157 nm, hydrophobicity.

1. Introduction

Polymers are considered as good sensing materials for a variety of applications [1-5] since they successfully meet the minimum requirements for fast response, sensitivity, repeatability and chemical selectivity. The definition of functionalized polymeric areas with different sensing properties is not compatible with standard industrial processes and is considered as a significant issue. For that reason, alternative methodologies, such as ink-jet printing, are usually applied for batch fabrication [6]. In this direction it has been shown that it is possible to fabricate a polymer arrays by applying conventional microelectronic processing steps [7] and this technology has been applied for the fabrication of gas sensor arrays based on polymer arrays on interdigitated electrodes [8]. The number of the areas with different sensing properties on the same substrate could be further increased by engineering of the already deposited polymer areas. Methodologies applied so far for the enhancement of detection efficiency and sensitivity are: a) Argon/Oxygen plasma processing [9] b) Ion implantation [10] and c) Excimer laser processing [11].

On the other hand, Vacuum UltraViolet (VUV) exposure (110-175 nm), has been proposed for the processing, functionalization and modification of the polymeric surfaces [12-14]. Chemical surface modification strongly depends on the VUV irradiation conditions, such as wavelength, intensity, energy and fluence of the light source and the ambient conditions. VUV irradiation alters the polymers structure by forming new radicals, which either further react with the ambient molecules such as oxygen followed by surface oxidation, or they recombine to form new stable intermediate bonds inside the polymeric chain, up to a certain depth from the surface, specified by the penetration depth of the VUV photons. The photo induced changes in the VUV in one hand, modulate the physical/ chemical functionality of the polymeric surfaces such as hydrophilicity, wetability, or biocompatibility and on the other hand, lead to surface modification with nano- resolution. In addition, modification of chemical composition and roughness of the irradiated part of the organic films is achieved, enhancing thus the surface-probe binding strength and the detection sensitivity in a predetermined way.

In this work, poly(methyl methacrylate) (PMMA) thin films are irradiated with laser light at 157 nm with the aim to enhance humidity detection sensitivity. The polymer modification due to VUV irradiation is responsible for large film thickness variation (swelling) during sorption of the analyte vapors. The swelling was monitored by the White Light Reflectance Spectroscopy (WLRS) methodology [15], successfully applied previously to measure the interaction kinetics of thin polymer films in a variety of applications [16, 17]. It was found that film swelling and thus detection sensitivity is increasing significantly (400%), when the PMMA films were processed at 157 nm. The unprocessed and processed PMMA films were further analyzed by XPS and AFM imaging. It was found that 157 nm irradiation forms new double carbon and carbonyl bonds and reduces accompanied by the re-

duction of carbon hydrogen bonding and subsequent carbonization. In addition, morphological changes of the polymer's surface in the nano/micro domain were observed increasing thus the film's porosity. The average size distribution in the nano/micro domain was dependent on the total laser fluence. Above threshold fluence, the relative volume expansion is non-linearly due to excessive carbonization of the polymer surface, which changes the surface morphology and structure. 157 nm laser treatment forms the basis to engineer a novel class of polymer sensor arrays with enhanced detection efficiency.

2. Experimental setup

PMMA with M_w=120K (Sigma-Aldrich) was selected, because PMMA with low molecular weights cannot withstand post exposure processing. The solution was prepared from PMMA polymer (6% w/w) in propyl glycol mether ether acetate (PGMEA) after 96 hours stirring and subsequent filtering. The substrates used were Si wafers, with 1 μm thick thermally grown SiO_2 layer (1100 ^oC, 200 min, and wet oxidation). The solution was spin coated on the SiO_2 layers and further baked on a hot plate at 160 ^oC for 60 min. The initial PMMA film thickness was ~220 nm. The set-up used for the monitoring of the film thickness variations due to water sorption, consists of the WLRS apparatus, a delivering subsystem for controlling the concentration of analytes and the working chamber where the sample films were placed. The WLRS methodology is based on the use of reflectance spectrum to calculate in real time the film thickness of the top layer (PMMA film in the present case). The thick SiO_2 layer provides the necessary interference fringes in the spectrum range monitored for accurate measurement of the temporal PMMA film thickness changes due to the absorption of analytes. The detection limit of thickness changes with the WLRS methodology is 0.2nm.

Dry high purity nitrogen flow was used in the analyte-delivering unit. Initially it was split into two parts, the carrier and the diluting part, by of two mass flow controllers. The carrier was bubbled through the compounds of interest and subsequently they mixed with the diluting part to achieve the required concentration level in the working chamber. The chamber volume was ~150 ml and the gas flow 1000 ml/min. The temperature in the gas delivering subsystem and in the working chamber was kept constant at 30 +/- 0.5^0C.

The experimental set-up for VUV exposure of the polymeric films consisted from the 157 nm molecular fluorine laser, (Lambda Physik, LPF 200), the all stainless steel vacuum chamber containing the computer-controlled X-Y-Z-θ translation stage where the polymer substrates were placed [18]. During the exposure procedure care was taken to avoid stray light falling on the chamber walls and on the components of the translation stage. The chamber was purged with high purity nitrogen. The nitrogen flow was controlled during the experiment and the ambient pressure was kept at 10^5 Pascal. The irradiation of the samples was performed at room temperature. The laser repetition rate was 15 Hz and the pulse duration was 15 ns at FWHM and the energy per pulse was adjusted at 5 mJ/cm^2. Samples have been irradiated at different fluence.

AFM imaging of the surface morphology of both non-irradiated and irradiated areas was performed using a ¨Quesant - Qscope 250¨. The AFM was equipped with a 40-μm Dual PZT scanner. Imaging was carried out with the NSC16 silicon cantilever. High-resolution images of the film surfaces were obtained at different scanning areas at a maximum scanning rate of 6 Hz and with image resolution 600x600 pixels. All AFM images were acquired in ambient conditions in intermittent contact mode.

The X-ray photoelectron spectroscopy (XPS or ESCA) analyses were carried out on the PHI-TFA XPS spectrometer (Physical Electronics Inc). The analyzed area was 0.4 mm in diameter and the analyzed depth was about 3 - 5 nm. Sample surfaces were excited by X-ray radiation from monochromatic Al source at photon energy of 1486.6 eV. High-energy resolution spectra C 1s and O 1s were acquired with energy resolution of about 0.6 eV with an analyzer pass energy of 29 eV on the surfaces of PMMA films in order to reveal binding energies of XPS peaks associated with different chemical states of elements. Due to sample charging the acquired XPS spectra were shifted by few eV on the energy scale. This effect was minimized by use of low-energy electron gun – neutralizer. In addition during data processing all C 1s spectra were aligned by setting the major C 1s peak at 285.0 eV, what is common procedure for XPS analysis on polymer films [13, 19] (The accuracy of binding energies was about ± 0.3 eV).

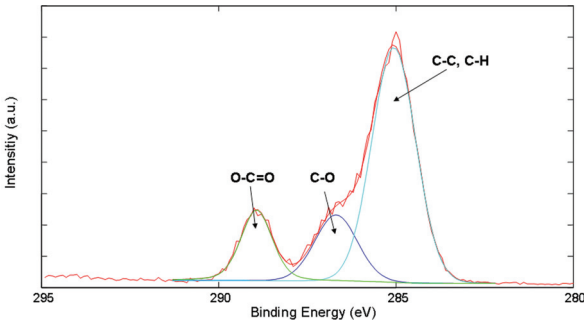

Fig. 1a C 1s XPS spectrum from the surface of the non-irradiated PMMA areas.

3. Results and Discussion

The photochemical effects following laser exposure of PMMA surfaces at 157 nm were investigated with XPS spectroscopy and AFM imaging and results are compared with previous studies of the same material using absorption VUV and UV spectroscopy [20-21]. Scission of polymeric bonds at 157 nm is followed by formation of new bonding. Additional processes such as stacking of photo dissociated moieties on the surface, formation of pillars, self assembly, volume or surface ablation, etc, [22] are tailoring further the surface functionality. The processes show such a degree of complexity, exhibiting spot size dependence [23].

From previous VUV –Vis absorbance studies the absorption bands below 160 nm were attributed to the $\sigma \rightarrow \sigma^*$ transitions of the C-C and C-H bonds, while the absorption band from around 180 nm was attributed to

the $\pi \rightarrow \pi^*$ transitions in the polymer chain [24,25]. The low intensity band around 275 nm is due to the $n \rightarrow \sigma^*$ transitions, and the band from 230 to 200 nm, is attributed to the $n \rightarrow \pi^*$ transitions of carbonyl chromophore groups [24]. In addition, the most typical absorption band for carbonyl compounds is spanning the wavelength range from 270 to 300 nm [25]. The spin coated PMMA samples on CaF_2 substrates were irradiated at 157 nm [26]. The most pronounced differences appears in the absorption spectra from 180 to 270 nm. The formation of carbon C=C double bonds in the main molecular chain and the formation of C=O groups in the side chains are the main changes recorded in the polymeric chain. Additionally, cross linking reactions are expected to take place after recombination of radicals following 157 nm exposure from the appearance of new bands [25]. The new chemical species are distributed on the surface of the PMMA polymer as deep as the penetration depth allows, (~500 nm in this experiment). Furthermore, the edge of the C-H absorption band was placed at 165 nm [27]. After the exposure at 157 nm, those bands are disappearing due to molecular photo-dissociation. The hydrogen of the main chain was dissociated and the structural changing was accompanied by free radical formation and cross linking (C-O-C bonding) as it is verified by the 190-200 nm absorption band [26].

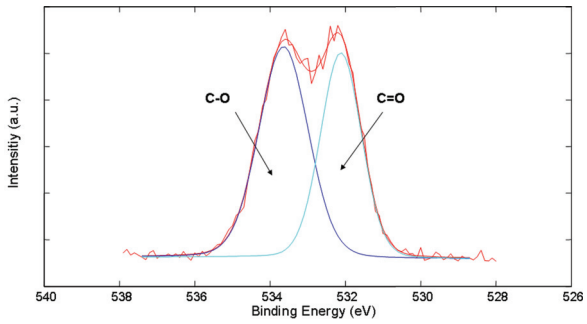

Fig. 1b O 1s XPS spectrum from the surface of the non-irradiated PMMA areas.

Using XPS analysis, the changes on the chemical structure induced by irradiation at 157 nm was further investigated. In Fig. 1a the C 1s XPS spectra from the surface of the initial non-irradiated sample is indicated. The C 1s peak of was decomposed by curve fitting into three components: the component at 285.0 eV corresponding to C-C and C-H bonds, the component at 286.5 eV corresponding to C-O bonds and the component at 288.9 eV corresponding to O-C=O bonds being in agreement with previously reported positions [13]. The O 1s peak Fig. 1b was decomposed, by curve fitting, into two components almost equal to each other components, the component at 532.1 eV corresponding to C=O bonds and the component at 533.6 eV corresponding to C-O bonds of the C=O-C of the PMMA unit.

In Fig. 2a a typical C 1s spectrum from the illuminated area of the sample at 157 nm is indicated. The sample was irradiated with 16.2 J/cm^2 total fluence (6 mJ/cm^2 pp). Comparing the C 1s spectra, of the non-irradiated/irradiated areas, the relative intensities of the C-O and C=O groups were significantly reduced after

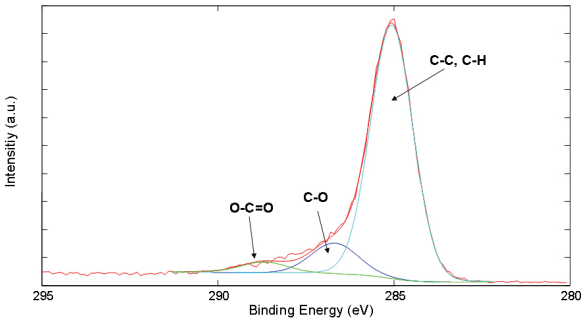

Fig. 2a C 1s XPS spectrum of the 157 nm irradiated area with 16.2 J/cm^2 total laser fluence (6 mJ/cm^2 pp).

157 nm laser irradiation, while the relative intensity of the C-C and C-H groups in the same spectra were higher. The peak increment can be attributed to cross-linking reactions and the formation of new C-C bonds. However since the XPS is unable to distinguish between the C-H, C-C and C=C bonds is not possible to identify the type of bonding. On the other hand from absorption measurements of [26], the C-H bonding disappears after irradiation. Therefore double bonding and cross linking reaction paths are following VUV irradiation. Furthermore the irradiation at 157 nm is accompanied by the loss of oxygen from the polymeric chain as it is confirmed by the decrease of the intensity of the respective peaks. The above results support the argument that under 157nm irradiation, the PMMA surface became carbon-rich and eventually it is expected to be hydrophobic as it has demonstrated in a series of previous experiments using VUV and UV absorption spectroscopy [26]. In Fig 2b the O 1 s spectra of the same irradiated area can be seen.

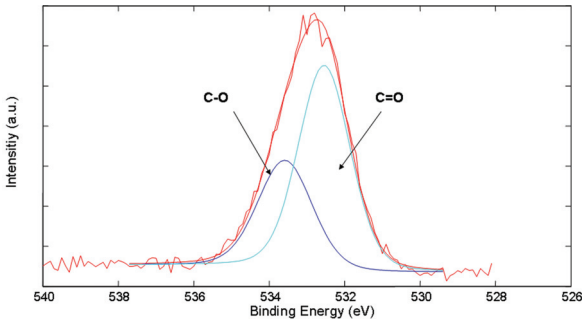

Fig. 2b O 1s XPS spectrum of the 157 nm irradiated area with 16.2 J/cm^2 total laser fluence (6 mJ/cm^2 pp).

After fitting the relative intensities of two peaks is different with the peak corresponding to C=O group to be higher than the one of the C-O group.

Smoothing of surfaces and development of regular structures with different physicochemical properties than the parent non-irradiated molecules regarding hydrophobicity and bio-compatibility, have been observed previously following VUV irradiation [28]. For revealing the mechanism of the 157 nm surface functionalization, the

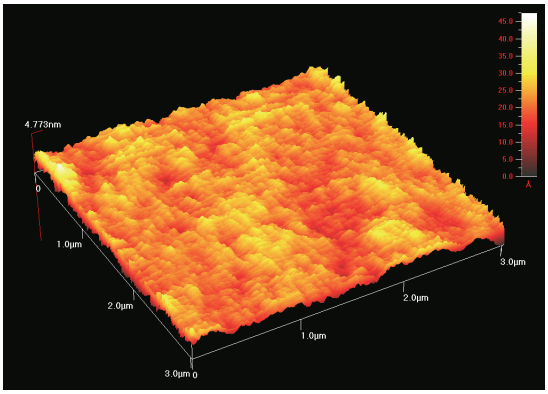

Fig. 3 AFM image of a non irradiated area of the PMMA film. The $Z_{av.}$ value is ~ 2.2 nm.

surface morphology of the non-exposed /exposed areas was imaged with AFM. Surface induced changes on polymers induced by VUV light in the nanoscale were imaged previously by AFM [13, 29,30]. In this experiment, the typical surface roughness of the non-irradiated areas (3 µm X 3 µm, AFM scanned area), was ~ 2.2 nm, Fig. 3. Following exposure with total fluence 0.27 J/cm^2, 0.1 mJ/cm^2 pp, the surface morphology of PMMA was changed significantly and distinct self assembled like

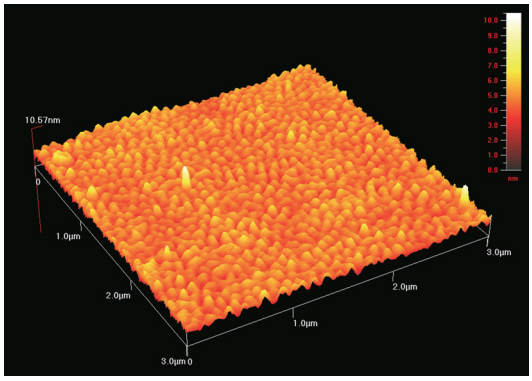

Fig. 4 AFM image of the PMMA film following 157 nm irradiation with 0.27 J/cm^2 total laser fluence. The $Z_{av.}$ value is 3.22 nm.

structures, 3 nm high and 100 nm wide were formed over the exposed area (3 µm X 3µm AFM scanned area), Fig. 4.

By further increasing the exposing time, Fig.5, the surface roughness over a 3 µm X 3 µm AFM scanned area was increased to ~ 12 nm. In addition the surface morphology indicates a high degree of organization as it can be seen on the 2D AFM image of Fig.6 where the distance between the vertical lines is 116 nm. The surface roughness histograms (z-direction) of non-exposed and exposed areas for a 3 µm X 3 µm are indicated in Fig.7. For the non-irradiated areas the surface roughness distribution is symmetric ~ 2 nm. The average surface roughness was increased to 3.2 nm and 12 nm respectively at higher irradiation fluence, Table 1. Z_{ave} is the average of the Z values within the given area; R_q (root mean square) is the standard deviation of the height values; Rp is the maximum height of the profile roughness above the mean plane; Rv is the lowest point bellow the mean image plane; Rt is the sum total of the maximum peak and maximum valley measurements. The surface parameters are increasing with increasing fluence. The scanned area was 3µm X 3µm. The results suggest that significant

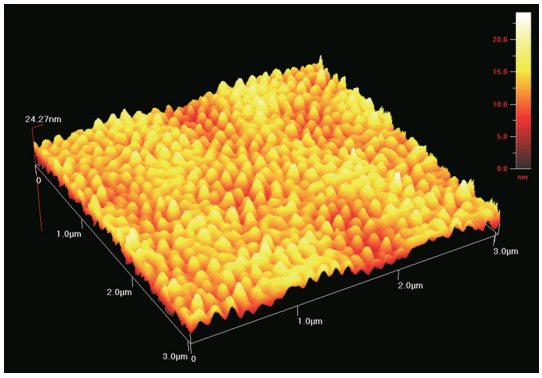

Fig. 5 AFM image of the PMMA film following 157 nm irradiation with 0.54 J/cm^2 total laser fluence. The $Z_{av.}$ value is 11.7 nm. The $Z_{av.}$ value is increasing at higher fluence.

morphological changes of the surface are induced with increasing the number of laser pulses at low laser fluence per pulse and at the same time the active surface area (porosity) of the polymeric material increases as well. At 157 nm, polymers are ablated only through photo chemical dissociation.

Film thickness variation of PMMA due to sorption (absorption / desorption) at different water (vapor) concentrations of (1000, 5000 and 10000 ppm) for the non-irradiated sample is indicated in Fig. 8. Following the experimental procedure, described above, the thickness variation of PMMA films of irradiated/ non-irradiated

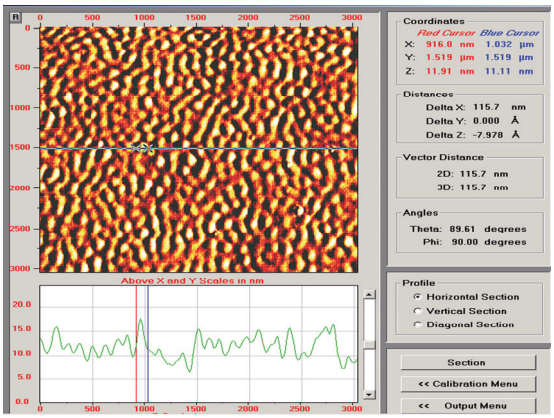

Fig. 6 2D AFM image of the PMMA film following 157 nm irradiation with 0.54 J/cm^2 total laser fluence. The average size of the self -assembled structures is 116nm.

areas due to humidity sorption was measured at different concentrations of 1000, 5000 and 10000 ppm respectively. The thickness variation of an exposed area (dynamic measurement) due to the sorption at different concentrations of humidity is indicated in Fig.9. The extend of the film swelling depends on the humidity concentration and the transition of the thickness variation from nitrogen (background) to the equilibrium under humidity is taking place within 90 sec in the case of 1000 ppm. When the

Table 1. Surface parameters of the irradiated areas at different irradiation fluence obtained by the analysis of the AFM images.

	0.00 J/cm^2	0.27 J/cm^2	0.54 J/cm^2
Z_{ave} (nm)	2.2	3.2	11.7
Rq (nm)	0.2	0.5	2.6
Rp (nm)	1.5	2.3	12.5
Rv (nm)	2.2	3.2	11.7
Rt (nm)	2.9	5.9	2.0

chamber was filled again with nitrogen, the water was desorbed from the PMMA film and the film thickness was attained the same value as prior to absorption. Thus the water molecules are fully desorbed from that particular polymer, indicating a weak polar bonding between the water and the polymer's chemical groups.

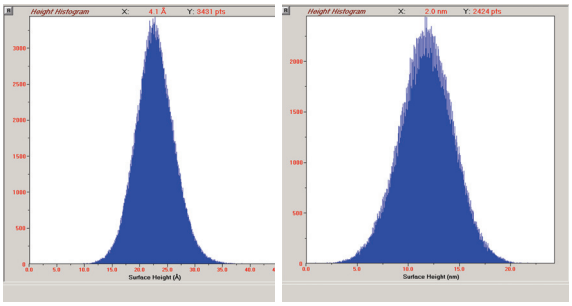

Fig. 7 Height histogram for a scan area of 3 μm X 3 μm. The left histogram is for the non irradiated area, and the Z_{av} value is 2.2 nm. The right histogram is for the irradiated area with total fluence of 0.54 J/cm^2. The $Z_{av.}$ value in this case is 11.7 nm.

The thickness variation after exposure at 22.55 J/cm^2 for various concentrations of water vapors (1000, 5000, 10000 ppm) is illustrated in Fig. 10. The film thickness of the irradiated sample was ~129 nm corresponding to a

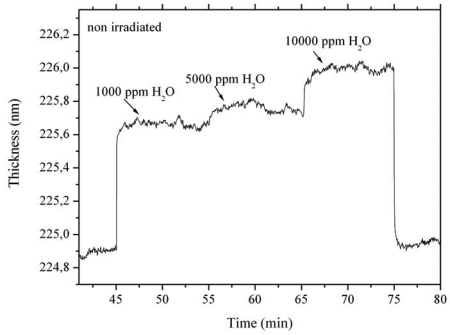

Fig. 8 Increment of film thickness of PMMA due to sorption (absorption / desorption) with different concentrations of water (vapor) (1000, 5000 and 10000 ppm) for the non-irradiated sample.

significant film thickness loss due to surface and volume ablation following VUV irradiation [27]. The absorption of water molecules within the polymer film is responsible for film thickness variation higher than of the non-irradiated samples. The time to reach equilibrium (1000 ppm), was estimated to be approximately 60 sec, while the desorption time was significantly longer (~240 sec).
Due to the thickness differences of the irradiated / non-irradiated samples, the sorption efficiency should be normalized and the relative film thickness variation

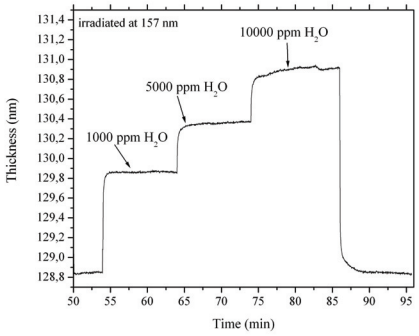

Fig. 9 Increment of film thickness of PMMA due to sorption (absorption / desorption) with different concentrations of water (vapor) (1000, 5000 and 10000 ppm) for the 157 nm irradiated sample (13.5 J/cm^2).

(swelling) at equilibrium $\Delta L/L_0$, depends on the analyte's concentration. L_0 is the polymer's film thickness prior to sorption and ΔL is the increment of polymer film thickness after sorption. The relative swelling values $\Delta L/L_0$ of

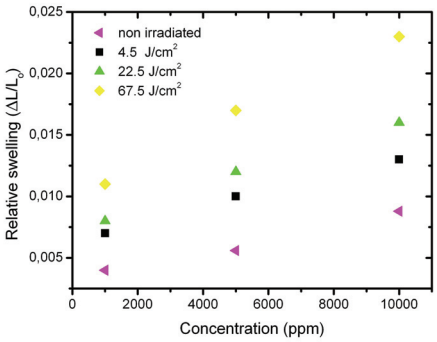

Fig. 10 Relative swelling values of PMMA for irradiated samples at different 157 nm exposure doses (4.5, 13.5, 22.5, 45, 67.5 J/cm^2) for water vapors. The relative swelling of the non-irradiated samples is indicated as well for comparison.

the polymeric films at equilibrium at high laser fluence, of 4.5, 22.5, and 67.5 J/cm^2 respectively and the relative swelling of the non-irradiated samples for water vapors is indicated in Fig. 10. For all the experimental cases, the swelling of the exposed samples was higher than of the non- irradiated ones. However, the relative swelling did not increased monotonically at higher fluence, a fact, which indicates that saturation is obtained due to saturation in film carbonization. The highest relative swelling value was observed for 67.5 J/cm^2. However at higher laser fluence the film surface morphology consists of areas with micro and nano- domain, in the X-Y direction, Fig. 11, but in this case the surface roughness does not increase significantly.
With the above experimental configuration, the chemical selectivity of water and methanol is of the same order of

magnitude. However, ethanol has 30 times higher selectivity than methanol and water [26].

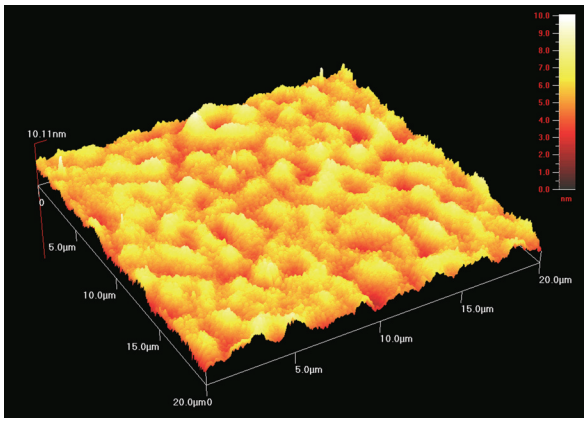

Fig.11 AFM image of the PMMA film following 157 nm irradiation with 67 J/cm^2 total laser fluence. Morphological changes are in the micro and nano domain having different shapes. The $Z_{av.}$ value is 11.7 nm.

Conclusions

PMMA thin films were processed with laser light at 157 nm. The irradiated films indicated enhanced swelling during water vapor absorption in comparison to the swelling of the non-irradiated films. The higher swelling was due to surface chemical modification and porosity increment following laser treatment. XPS and AFM imaging indicate enhanced carbonization and porosity of the illuminating areas. The irradiated polymer becomes more hydrophobic causing relatively higher swelling in comparison to the non-irradiated areas.

References

[1] B. Adhikari, and S. Majumdar: Prog. Polym. Sci., 29, (2004) 699.
[2] R. Capan , A. K. Ray , T. Tanrisever, and A. K. Hassan: Smart Mater. Struct., 14, (2005) 11.
[3] R. Capan, A. K. Ray, A. K. Hassan, and T. Tanrisever: J. Phys. D: Appl. Phys., 36, (2003) 1115.
[4] M. Garcia, M.J. Fernandez, J.L. Fontecha, J. Lozano, J.P. Santos, M. Aleixandre, I. Sayago, J. Gutierrez, and M.C. Horrillo: Talanta, 68, (2006) 1162.
[5] A. Guadarrama, J.A. Fernández, M. Íñiguez, J. Souto, and J.A. de Saja: Anal. Chim. Acta, 411, (2000) 193.
[6] L. Setti, A. Fraleoni-Morgera, B. Ballarin, A. Filippini, D. Frascaro, and C. Piana: Biosens. Bioelectron., 20, (2005) 2019.
[7] M. Kitsara, D. Goustouridis, S. Chatzandroulis, K. Beltsios, and I. Raptis: Microelectron. Eng., 83, (2006) 1192.
[8] M. Kitsara, D. Goustouridis, S. Chatzandroulis, M. Chatzichristidi, I. Raptis, Th. Ganetsos, R. Igreja, and C.J. Dias: Proc. Eurosensors, Göteborg, (2006) T1-P24.
[9] J.F. Friedrich, W.E.S. Unger, A. Lippitz, I. Koprinarov, G. Kühn, St. Weidner, and L. Vogel: Surf. Coat. Tech., 116/119, (1999) 772.
[10] M. Guenther, G. Gerlach, G. Suchaneck, K. Sahre, K.J. Eichhorn, V. Baturin, and S. Duvanov: Nucl. Instrum. Meth. B, 216, (2004) 143.
[11] W. Pfleging, M. Przybylski, and H.J. Brückner, Proc. SPIE, 6107, (2006) 61070G.
[12] A.M. Douvas, P.S. Petrou, S.E. Kakabakos, K. Misiakos, P. Argitis, E. Sarantopoulou, Z. Kollia, and A.C. Cefalas: Anal. Bioanal. Chem., 381, (2005) 1027.
[13] A. Hozumi, N. Shirahata, Y. Nakanishi, S. Asakura, and A. Fuwa: J. Vac. Sci. Technol. A, 22, (2004) 1309.
[14] T. Lippert, and J.T. Dickinson: Chemical Reviews, 103, (2003) 453.
[15] N. Vourdas, G. Karadimos, D. Goustouridis, E. Gogolides, A.G. Boudouvis, J.-H. Tortai, K. Beltsios, and I. Raptis: J. Appl. Polym. Sci., 102, (2006) 4764.
[16] K. Manoli, D. Goustouridis, S. Chatzandroulis, I. Raptis, E.S. Valamontes, and M. Sanopoulou: Polymer, 47, (2006) 6117.
[17] M. Zavali, P.S. Petrou, S.E. Kakabakos, M. Kitsara, I. Raptis, K. Beltsios, and K. Misiakos: IEE Micro Nano Lett., 1, (2006) 94.
[18] E. Sarantopoulou, Z. Kollia, K. Koevar, I. Muevi, S. Kobe, G. Drai, E. Gogolides, P. Argitis, and A. C. Cefalas: Mater. Sci. Engin. C, 23, (2003) 995.
[19] A. Hozumi, T. Masuda, H. Sugimura, and T. Kameyama: Langmuir, 19, (2003) 7573.
[20] F. E. Truica Marasescu, and M. R. Wertheimer: Macromol. Chem. Phys., 206, (2006) 744.
[21] S. Onari: J. Phys. Soc. Jpn, 26, (1969) 500.
[22] Z. Kollia, E. Sarantopoulou, A. C. Cefalas, S. Kobe, P. Argitis, and K. Missiakos: Appl. Surf. Sci., 248, (2005) 248.
[23] D. Riedel, and M. C. Castex: Appl. Phys. A, 69, (1999) 375.
[24]A.C. Fozza, J.E. Klemberg – Sapieha, and M.R. Wertheimer:Plasmas Polym., 4, (1999) 183.
[25] V.E. Skurat, and Y.I. Dorofeev: Angewandte Makromolekulare Chemie, 216, (1994) 205.
[26] E. Sarantopoulou, Z. Kollia, A. C. Cefalas, K. Manoli, M. Sanopoulou, D. Goustouridis, S. Chatzandroulis, and I. Raptis: Accepted for publication in Appl. Surf. Science (2007). Doi:10.1016/apsusc.2007.07.138
[27] J.J. Pireaux, J. Riga, R. Caudano, and J. Verbist: Am. Chem. Soc. Symp. Proc., 162, (1981) 169.
[28] V.N. Vasilets, A.V. Kuznetsov, and V.I. Sevastianov: J. Biom. Mat. Res. Part A, 69, (2004) 428.
[29] M. Nowicki, H. Kaczmarek R. Czajka, and B. Susa: J. Vac. Sci. Technol. A, 18, (2000) 2477.
[30] A. Hozumi, T. Masuda, K. Hayashi, H. Sugimura, O. Takai, and T. Kameyama: Langmuir, 18, (2002) 9022.

(Received: April 24, 2007, Accepted: September 14, 2007)